J|A|C|S COMMUNICATIONS

Published on Web 09/09/2009

Hetero-Epitaxial Anion Exchange Yields Single-Crystalline Hollow Nanoparticles

Jungwon Park,[†] Haimei Zheng,[†,‡,§] Young-wook Jun,[†,§] and A. Paul Alivisatos*[,†,§]

Department of Chemistry, University of California, Berkeley, California 94720, National Center for Electron Microscopy, Lawrence Berkeley National Laboratory, Berkeley, California 94720, and Materials Science Division, Lawrence Berkeley National Laboratory, Berkeley, California 94720

Received July 10, 2009; E-mail: alivis@berkeley.edu

In recent years, chemical transformation of inorganic solids has emerged as an attractive approach for nanostructure synthesis.[1,2] In addition to its utility in generating various nanoparticle materials, ranging from metal to semiconductor and to magnetic nanoparticles, this method has enabled the fabrication of new types of nanostructures with high compositional and structural complexity. For example, thermodynamically unfavorable hollow particles have been synthesized using chemical transformations, by exploiting the nanoscale Kirkendall effect[2−5] and nonequivalent stoichiometry[6−8] between solid 'precursor' nanoparticles and the incoming molecular species. Moreover, ion exchange of inorganic solids has proven an effective tool for chemical transformation of nanoparticles.[9−11] For example, we recently reported that the addition of cations into a binary semiconductor nanoparticle solution induces conversion of the initial nanoparticle into another chemical species.[9,12,13] The resulting nanoparticles are both highly crystalline and characterized by size and shape monodispersity. Nanoscale heterojunctions[12] and barcodes[13] could further be fabricated by varying the ion concentration.

In the examples mentioned above, rapid cation motion strongly influences the final composition and geometry. In the present work, we examine a case of anion rather than cation exchange. The most prominent example of anion exchange in a nanoscale system is for the ZnO/ZnS system. Schaak et al. have recently examined the case as well as Dloczik and Konenkamp.[10,14] We study the anion exchange of ZnO nanoparticles with molecular sulfur precursors to form high quality ZnS nanoparticles. Although there have been reports on anion exchange reactions of binary compound semiconductor nanoparticles (including Cu_7S_4,[15] ZnSe,[16] and AlN[17]), our study can be differentiated from previous research in the following regards: (*i*) We find that the anion exchange of ZnO with sulfur molecules is accompanied by the nanoscale Kirkendall effect, yielding hollow structures rather than solid nanoparticles. Interestingly, the overall transformed morphology mimics the initial nanoparticle shape. (*ii*) The resulting ZnS nanoparticles are single crystalline and preserve the crystal symmetry and orientation of the initial ZnO nanoparticles. Note that chemical transformation of nanoparticles accompanied by the Kirkendall effect often results in polycrystalline nanoparticle products; single-crystalline hollow structures are rarely obtained.[10,18,19] In a recent study, single-crystalline hollow nanorods including Ni_3Sn_4 and PtSn have been produced by using Sn nanoparticles as a template.[20] Highly crystalline $ZnAl_2O_4$ nanotubes were also fabricated *via* a thermal annealing process of ZnO−Al_2O_3 coaxial nanowires.[21] However, this method required relatively high temperatures (∼700 °C), and the fabricated nanotubes still exhibited crystallographically random orientations and grain boundaries. (*iii*) We use both crystallographic and compositional analyses of partially converted intermediate yolk−shell particles to understand the shape and crystallographic retention properties of our ZnS hollow nanoparticles. These analyses yield further insight into the mechanisms of the chemical transformations.

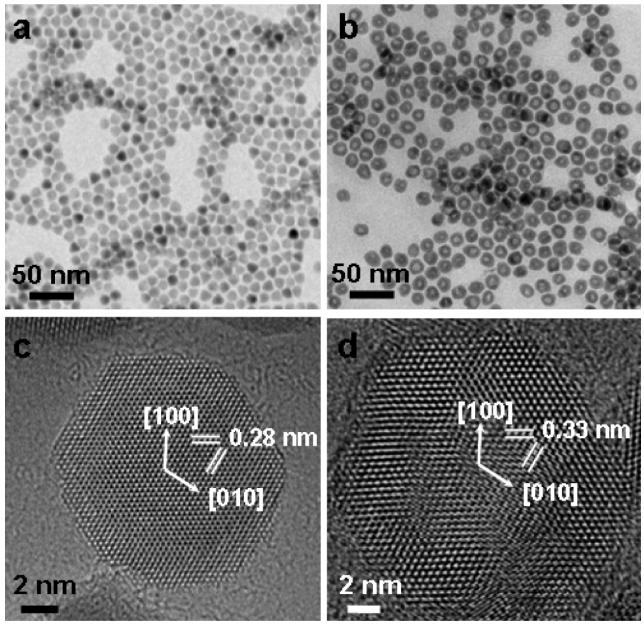

Figure 1. TEM and HRTEM images of initial ZnO nanoparticles (a, c) and ZnS hollow nanoparticles obtained after anion exchange (b, d).

Anion exchange of ZnO nanoparticles was performed using the following procedure: single-crystalline, hexagonal pyramid shaped ZnO nanoparticles (the diagonal distance of the hexagonal surface is 14 nm) (Figure 1a, c) were mixed with 5 g of trioctylphosphine oxide under Ar gas and heated to 235 °C. Hexamethyldisilathiane (26 mg) in trioctylphosphine (2 g) was added dropwise for 80 min. After 15 min, the reaction flask was cooled to room temperature, washed with acetone, and centrifuged several times to isolate nanoparticles as white precipitates. Additional details of synthetic protocol can be found in the Supporting Information.

When ion exchange of binary semiconductors is initiated on the surface, further exchange reaction requires diffusion of ionic reactants. Two possible scenarios may be identified: (*i*) New ions diffuse inward to the parent nanoparticle continuously, resulting in a directional migration of the reaction interface toward the core. A cation exchange reaction is such an example. (*ii*) Inward ion diffusion is limited and core species diffuse outward, generating a

[†] University of California, Berkeley.
[‡] National Center for Electron Microscopy, Lawrence Berkeley National Laboratory.
[§] Materials Science Division, Lawrence Berkeley National Laboratory.

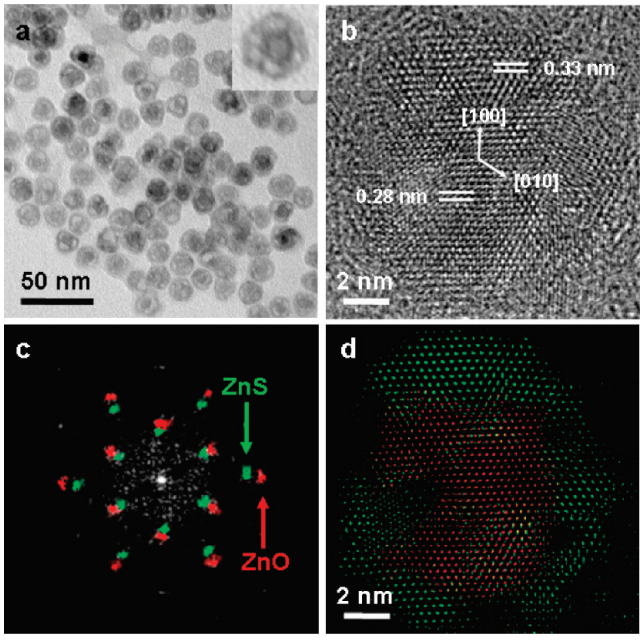

Figure 2. (a) TEM image of partially exchanged yolk−shell nanoparticles. (b) HRTEM image of a single yolk−shell nanoparticle. (c) FFT of (b). (d) Reconstructed crystal structure from (c) (red: ZnO, green: ZnS; see Supporting Information for original images).

void space inside the nanoparticle. Interestingly, unlike cation exchange reactions, the anion exchange of ZnO nanoparticles with molecular sulfur precursors follows the latter case, described in detail below.

Figure 1b shows a transmission electron microscope (TEM) image of the ZnS nanoparticles obtained. Similar to the parent ZnO nanoparticles, ZnS nanoparticles exhibit hexagonal pyramid geometry (see Supporting Information), but each nanoparticle has a single pore in its interior. So far, we have seen many cases where cation diffusion is much faster than anion diffusion.[3,6,9,12,13] The present case is also of this type where Zn^{2+} cations diffuse faster than incoming S^{2-}, so that even though anion exchange is taking place, it is the cation diffusion that controls the final morphology. In addition to fast diffusion of Zn^{2+}, faster diffusion of O^{2-} than incoming S^{2-} leads to the formation of a hollow structure from the anion exchange reaction. High-resolution TEM (HRTEM) and energy filtered TEM (EFTEM) (Figure 1, Supporting Information) experiments support the complete conversion of the initial nanoparticles into ZnS hollow nanoparticles. Most notably, the ZnS nanoparticle shells are a single-crystalline wurtzite structure, identical to the crystal structure of the initial ZnO nanoparticles.

Structural analyses of partially exchanged yolk−shell nanoparticles provide important clues to the origin of the shape and crystallographic similarities of the ZnS nanoparticles with the initial ZnO. These partially exchanged nanoparticles have voids between the ZnO core and ZnS shell (Figure 2a). In addition, some nanoparticles have bridges interconnecting the ZnO core with the outer ZnS. These bridges serve as transport pathways for the ZnO core (Figure 2a, inset).[22] HRTEM images (Figure 2b) indicate two sets of epitaxially aligned hexagonal fringes at the core and shell regions, corresponding to ZnO and ZnS lattice structures, respectively. Such heteroepitaxial features are clearly confirmed by two well-aligned sets of hexagonal spots in the fast-Fourier transform (FFT) of the HRTEM image (Figure 2c). In addition, the reconstructed image from both sets of spots confirms epitaxially grown yolk−shell particles (Figure 2d). These observations indicate that formation of single-crystalline ZnS is possible through heteroepitaxial ZnO@ZnS intermediates during the anion exchange. It is noteworthy that bulk heteroepitaxy between these two materials is not favored because of the high strain energy at the interface due to relatively large lattice mismatches.

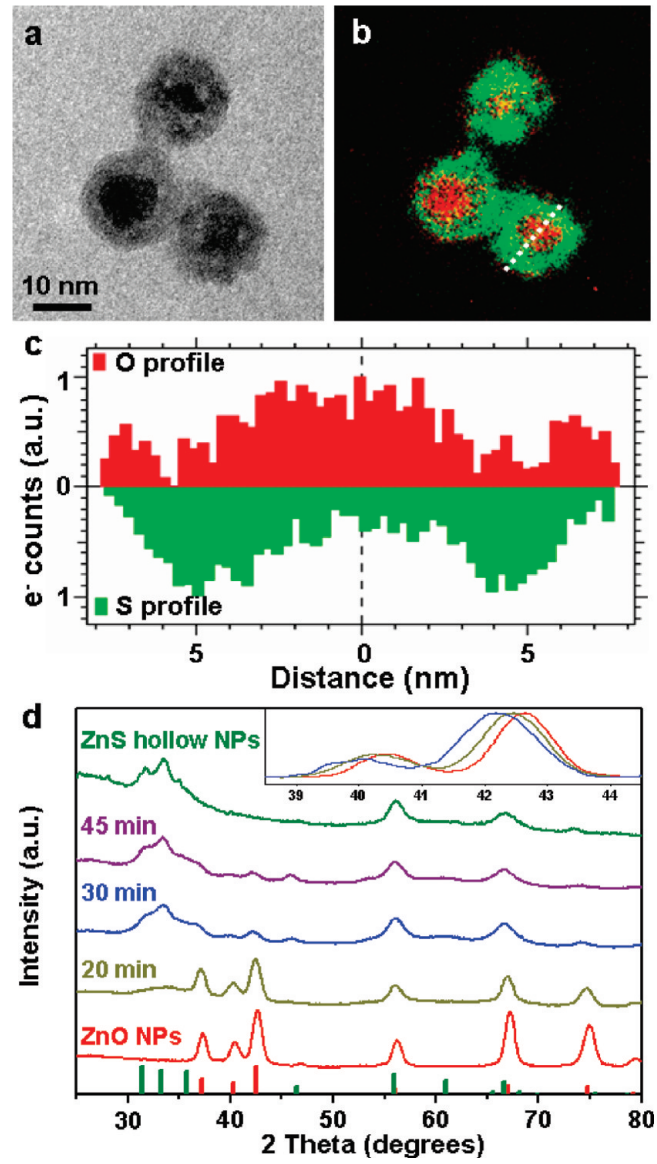

Figure 3. TEM (a) and EFTEM images (b) of the partially exchanged yolk−shell nanoparticles (red: O map, green: S map; see Supporting Information for original images). (c) Oxygen and sulfur line profiles along the cross section in (b). (d) XRD patterns of the nanoparticles at different stages of anion exchange reaction from initial ZnO (red) to final ZnS hollow (green) via intermediates (yellow, blue, and purple). Inset: Magnified and normalized patterns from $2\theta = 38.5°$ to 44.5°.

We performed additional composition analyses of partially converted yolk−shell intermediates using EFTEM analyses with oxygen and sulfur windows. The results provide insight about the release of lattice strain during the heteroepitaxial anion exchange reaction. Color mapped EFTEM images (Figure 3b) of partially converted yolk−shell nanoparticles (Figure 3a) and line profiles (Figure 3c) clearly show the presence of O and S at the core and shell, respectively. Interestingly, the oxygen signal also appears in the shell region. This observation supports the hypothesis that oxygen diffuses out of the core nanoparticles and is accumulated in the shell region before the anion exchange with sulfur precursors. Consistently, as the anion exchange reaction proceeds, a gradual

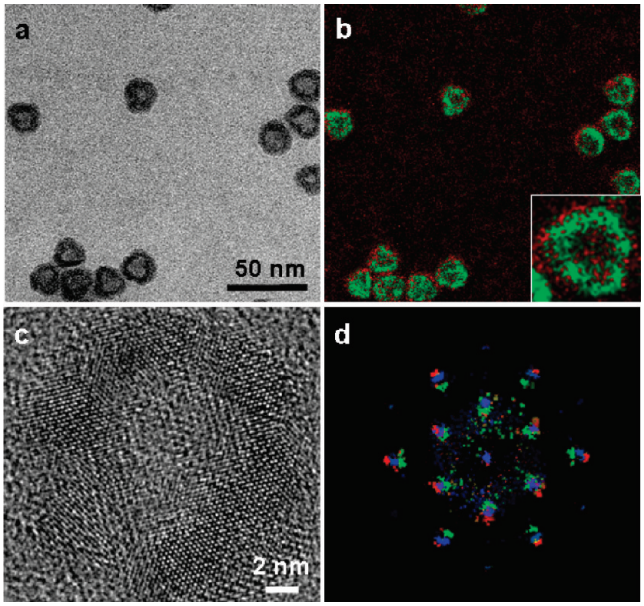

Figure 4. TEM image (a), EFTEM image (b) with magnified inset, and HRTEM image (c) for thermally annealed yolk−shell intermediate nanoparticles. (d) FFT image of Figure 4c overlaid in Figure 2c (red: ZnO, green: ZnS, blue: the thermally annealed intermediate nanoparticle; see Supporting Information for original images).

shift of the initial ZnO X-ray diffraction (XRD) peaks to lower angles supports the presence of mixed $ZnO_{1-x}S_x$ intermediate species (see also Supporting Information).

In fact, once the ZnS shell forms, outward oxygen diffusion spontaneously proceeds without the help of further anion exchange. Figure 4a shows a TEM image of nanoparticles obtained after thermal treatment of partially converted yolk−shell without sulfur precursors. Synthetic protocol for thermal treatment can be found in the Supporting Information. Core ZnO nanoparticles have disappeared in the TEM and EFTEM (Figure 4b) images, but oxygen signals now appear in the shell region. HRTEM images (Figure 4c) and their corresponding FFTs (blue spots in Figure 4d) indicate that the shell now forms ZnO_xS_{1-x} alloys as a result of ZnO diffusion into ZnS shells.

From our structural and composition analyses of partially and fully converted nanoparticles, we propose the following anion exchange reaction mechanism: initially, thin layers of ZnS grow epitaxially onto the ZnO core through the surface anion exchange reaction, which generate a highly strained interface between the ZnO core and the ZnS shell. To release this interface energy, the ZnO core spontaneously diffuses into the ZnS shell, which is finally exchanged with sulfur precursors at the outer shell surface, forming fully converted ZnS hollow nanoparticles.

In summary, we have demonstrated anion exchange of binary ZnO semiconductor nanoparticles. Unlike cation exchange, the anion exchange is accompanied by the nanoscale Kirkendall effect, yielding hollow nanoparticles. Parent-particle shape, single crystallinity, and orientation of the transformed particles are completely preserved through this heteroepitaxial anion exchange reaction. Our anion exchange can be extended to other binary or tertiary nanoparticles, to produce high quality, single crystalline hollow nanoparticles.

Acknowledgment. This work was supported by the Director, Office of Science, Office of Basic Energy Sciences, Materials Sciences and Engineering Division, of the U.S. Department of Energy under Contract No. DE-AC02-05CH11231 for funding the development of a new synthetic approach for the hollow nanomaterials and by a grant from DAF AFOSR under Award No. FA9550-07-1-0334 for the examination of the nanomaterials for energy absorbing properties. Helpful discussions with and revision by Jennifer A. Dionne are acknowledged. TEM investigation was performed at National Center for Electron Microscope, LBNL.

Supporting Information Available: Experimental conditions, characterization methods, tilting TEM images, EFTEM images of ZnS, original images of figures discussed above, reconstruction process of FFT, and calculated alloy composition after thermal treatment. This material is available free of charge via the Internet at http://pubs.acs.org.

References

(1) Vasquez, Y.; Henkes, A. E.; Bauer, J. C.; Schaak, R. E. *J. Solid State Chem.* **2008**, *181*, 1509–1523.
(2) Fan, H. J.; Gosele, U.; Zacharias, M. *Small* **2007**, *3*, 1660–1671.
(3) Yin, Y. D.; Rioux, R. M.; Erdonmez, C. K.; Hughes, S.; Somorjai, G. A.; Alivisatos, A. P. *Science* **2004**, *304*, 711–714.
(4) Yin, Y. D.; Erdonmez, C. K.; Cabot, A.; Hughes, S.; Alivisatos, A. P. *Adv. Funct. Mater.* **2006**, *16*, 1389–1399.
(5) Wang, Y. L.; Cai, L.; Xia, Y. N. *Adv. Mater.* **2005**, *17*, 473.
(6) Sun, Y. G.; Xia, Y. N. *Science* **2002**, *298*, 2176–2179.
(7) Sun, Y. G.; Xia, Y. N. *J. Am. Chem. Soc.* **2004**, *126*, 3892–3901.
(8) Selvakannan, P. R.; Sastry, M. *Chem. Commun.* **2005**, 1684–1686.
(9) Son, D. H.; Hughes, S. M.; Yin, Y. D.; Alivisatos, A. P. *Science* **2004**, *306*, 1009–1012.
(10) Dloczik, L.; Konenkamp, R. *Nano Lett.* **2003**, *3*, 651–653.
(11) Kovalenko, M. V.; Talapin, D. V.; Loi, M. A.; Cordella, F.; Hesser, G.; Bodnarchuk, M. I.; Heiss, W. *Angew. Chem., Int. Ed.* **2008**, *47*, 3029–3033.
(12) Sadtler, B.; Demchenko, D. O.; Zheng, H.; Hughes, S. M.; Merkle, M. G.; Dahmen, U.; Wang, L.-W.; Alivisatos, A. P. *J. Am. Chem. Soc.* **2009**, *131*, 5285–5293.
(13) Robinson, R. D.; Sadtler, B.; Demchenko, D. O.; Erdonmez, C. K.; Wang, L. W.; Alivisatos, A. P. *Science* **2007**, *317*, 355–358.
(14) Dawood, F.; Schaak, R. E. *J. Am. Chem. Soc.* **2009**, *131*, 424–425.
(15) Cao, H. L.; Qian, X. F.; Wang, C.; Ma, X. D.; Yin, J.; Zhu, Z. K. *J. Am. Chem. Soc.* **2005**, *127*, 16024–16025.
(16) Geng, J.; Liu, B.; Xu, L.; Hu, F. N.; Zhu, J. J. *Langmuir* **2007**, *23*, 10286–10293.
(17) Zhang, Q. H.; Gao, L. *J. Am. Ceram. Soc.* **2006**, *89*, 415–421.
(18) Shao, H. F.; Qian, X. F.; Zhu, Z. K. *J. Solid State Chem.* **2005**, *178*, 3522–3528.
(19) Lin, M.; Zhang, J.; Boothroyd, C.; Foo, Y. L.; Yeadon, M.; Loh, K. P. *J. Phys. Chem. B* **2004**, *108*, 9631–9637.
(20) Chou, N. H.; Schaak, R. E. *Chem. Mater.* **2008**, *20*, 2081–2085.
(21) Fan, H. J.; Knez, M.; Scholz, R.; Nielsch, K.; Pippel, E.; Hesse, D.; Zacharias, M.; Gosele, U. *Nat. Mater.* **2006**, *5*, 627–631.
(22) Fan, H. J.; Knez, M.; Scholz, R.; Hesse, D.; Nielsch, K.; Zacharias, M.; Gosele, U. *Nano Lett.* **2007**, *7*, 993–997.

JA905732Q